Dynamic hip kinematics before and after periacetabular osteotomy in patients with dysplasia

吉本，憲生
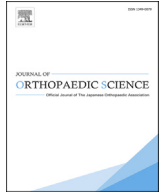
Original Article

Dynamic hip kinematics before and after periacetabular osteotomy in patients with dysplasia

Kensei Yoshimoto [a], Satoshi Hamai [a, *], Hidehiko Higaki [b], Hirotaka Gondoh [c],
Kyohei Shiomoto [a], Satoru Ikebe [d], Daisuke Hara [a], Keisuke Komiyama [a],
Yasuharu Nakashima [a]

[a] Department of Orthopedic Surgery, Graduate School of Medical Sciences, Kyushu University, 3-1-1 Maidashi, Higashi-ku, Fukuoka, 812-8582, Japan
[b] Department of Life Science, Faculty of Life Science, Kyushu Sangyo University, 2-3-1 Matsugadai, Higashi-ku, Fukuoka, 813-0004, Japan
[c] Department of Biorobotics, Faculty of Engineering, Kyushu Sangyo University, 2-3-1 Matsugadai, Higashi-ku, Fukuoka, 813-0004, Japan
[d] Department of Creative Engineering, National Institute of Technology, Kitakyushu College, 5-20-1 Shii, Kokuraminami-ku, Kitakyushu, Fukuoka, 802-0985
Japan

ARTICLE INFO

ABSTRACT

Background: We prospectively analyzed the hip kinematics in patients with developmental dysplasia of the hip (DDH) before and after periacetabular osteotomy (PAO) and in healthy subjects while squatting to determine the influence of coverage of the femoral head on hip kinematics.

Methods: 14 hips in 14 patients with DDH and 10 hips in 10 volunteers were included. Continuous radiographs while squatting and computed tomography images were obtained to assess the *in vivo* kinematics of the hip and the rim-neck distance using density-based 3D-to-2D model-to-image registration techniques.

Results: The maximum hip flexion angles were 100.4° and 94.9° before and after PAO (p = 0.0863), respectively. The maximum hip flexion angles after PAO did not significantly differ from those of normal hips (102.2°; p = 0.2552). The hip abduction angles at maximum hip flexion were 31.7° and 26.2° before and after PAO (p = 0.1256), respectively. The rim-neck distance decreased from averaged 12.2 mm −8.9 mm (p = 0.0044) after PAO. The lateral center edge angle (LCEA) and anterior center edge angle (ACEA) significantly improved 14.7°−42.4° and 50.4°−54.0° after PAO (p < 0.0001, p = 0.0347), respectively; in particular, the ACEA after PAO did not significantly differ from that in the normal hips (p = 0.1917). The ACEA was not correlated with hip flexion, or the rim-neck distance (p = 0.9601, 0.8764). The LCEA was also not correlated with hip abduction (p = 0.1683).

Conclusion: Patients after PAO showed no significant difference in maximum hip flexion while squatting compared to before PAO and normal hips. Horizontalized weight-bearing acetabulum with normalized ACEA could be adequate correction of the acetabular fragment to restore hip RoM without coxalgia that induce the inability to perform squats after PAO.

© 2019 The Japanese Orthopaedic Association. Published by Elsevier B.V. All rights reserved.

1. Introduction

Developmental dysplasia of the hip (DDH) is a common cause of secondary osteoarthritis (OA) [1]. Periacetabular osteotomy (PAO), including transposition osteotomy of the acetabulum [2–6], is an effective treatment for DDH. There are several variations in surgical technique [2,7–12], PAO can improve the acetabular coverage of the femoral head and restore joint congruity and stability. Previous studies have shown satisfactory intermediate to long-term outcomes of PAO with excellent deformity correction, pain relief, and restored function [8,10,13]. We also previously reported the survival rate in cases with total hip arthroplasty (THA) conversion or progress to the end stages of OA as 94% and 88% at 10 and 15 years after PAO [4].

Several recent reports have described the occurrence of secondary femoroacetabular impingement (FAI) after PAO [14–16]. This condition can result from the overcorrection of the acetabulum

* Corresponding author. Department of Orthopaedic Surgery, Kyushu University, 1-3-3 Maidashi, Higashi-ku, Fukuoka, 812-8582, Japan. Fax: +81 92-642-5507.
 E-mail address: hamachan@ortho.med.kyushu-u.ac.jp (S. Hamai).

and native cam type deformity of the proximal femur. Several computed tomography (CT) based simulation studies have also shown that hip flexion, abduction, and internal rotation decreased after PAO [17–19]. In particular, the anterior center-edge angle (ACEA) was found to have a negative correlation with flexion and internal rotation even in cases where the coverage of the femoral head was appropriate [17]. However, these simulation studies were performed *in vitro,* and they only considered the influence of bone morphology. Further *in vivo* analysis during daily activities such as deep hip flexion is needed to understand the dynamic kinematics in DDH and the influence of the coverage of the femoral head.

In this study, we aimed to evaluate (1) the kinematics of the hips between healthy subjects, patients before PAO, and after PAO, while squatting, using density-based 3D-to-2D model-to-image registration techniques [20–23]. We verified the hip kinematics, including maximum hip flexion, adduction/abduction, internal/external rotation, and distance between the acetabular rim and femoral neck at maximum hip flexion (rim-neck distance) [22,23], and then evaluated (2) whether the anterior and/or lateral coverage of the femoral head was significantly related to the hip range of motion (RoM) and rim-neck distance while squatting. We hypothesized that the amount of anterior and lateral acetabular coverage could significantly influence hip RoM while squatting.

2. Materials and methods

2.1. Subjects

From August 2012 to December 2015, total of 32 hips of 29 patients underwent PAO for symptomatic DDH by the experienced hip surgeons, Y.N. and S.H. The indications for the osteotomy were radiological evidence of dysplasia with Wiberg's lateral center-edge angle (CEA) of <20° [24], and hip pain that interfered with daily life. In this study, we could include 14 hips of 14 patients who agreed to participate in this study prior to surgery and met the following inclusion criteria: no neuromuscular disorders; no previous surgery of the hip and spine. Patients who were unable to squat safely without assistance before and after the operation, or had undergone THA during postoperative follow-up were excluded from the study; thus, no hips were excluded. We also included 10 normal hips of 10 subjects for comparison. The inclusion criteria for normal hips were the absence of any hip injury or surgery, and the absence of any abnormity in radiographic images of the hips. Among the 14 patients, 3 were male and 11 were female with an average age at surgery of 34.9 years (range, 13–57) and body mass index (BMI) of 23.5 kg/m^2 (range, 18.0–28.5). All dysplastic hips were categorized as Crowe 1 [25]. According to the category of dysplasia severity [26], 7 hips were classified as borderline-mild DDH (15° ≤ lateral CEA < 25°), 4 hips were classified as moderate DDH (5° ≤ lateral CEA < 15°), and 3 hips were classified as severe DDH (lateral CEA < 5°). The healthy subjects included 6 males and 4 females, with an average age of 30.7 years (range, 24–36) and BMI of 21.0 kg/m^2 (range, 17.0–26.1). There were no significant differences in age, gender and BMI between cases with DDH and normal hips (p = 0.3651, p = 0.0529 and 0.1783 respectively). Informed consent was obtained from all the subjects prior to participation in the study, which was approved by the Institutional Review Board. Radiographic images of the patients with DDH were obtained before PAO and one year after PAO.

2.2. Surgical technique

The procedure has been previously described in detail [2–6]. In brief, the patient is placed in the lateral decubitus position. A lateral approach with and without transtrochanteric osteotomy was used

in 3 and 11 cases, respectively. A spherical osteotomy is performed, starting 20 mm proximal to the superior acetabular edge and passing through the midpoint between the greater sciatic notch and the posterior edge of the acetabulum and the innominate sulcus of the ischium. Thereafter, a pubic osteotomy is performed lateral to the iliopubic tubercle. The acetabular fragment is rotated laterally to horizontalize weight-bearing acetabulum and improve anterior coverage, as well as medialization and distalization of the femoral head in case of subluxation. Although the majority of patients with DDH present with anterolateral acetabular deficiencies, previous studies have shown the acetabular version and the quantity and location of acetabular deficiencies can vary among individuals [9,27–30]. Therefore, anterior rotation of the acetabular fragment can exacerbate posterior acetabular coverage and therefore should be avoided in patients with insufficient posterior acetabular coverage [30–32]. We preoperatively evaluated the morphologic features of the hip of each patient three-dimensionally and customized the correction in accordance with the individual variation [29–31,33]. During procedure, we judged the amount of lateral rotation and anteversion of the fragment by reference to the 2.0 mm K-wire inserted in the fragment before correction, with intraoperative radiograph.

Active range of hip exercises and partial weight-bearing on two crutches were initiated one and two weeks after the surgery, respectively. Weight-bearing was gradually increased during postoperative rehabilitation, based on the extent of pain in the patients, whereas full weight-bearing was permitted five to eight weeks after the operation. No patients claimed the symptom of coxalgia with deep hip flexion or impingement test that limited the ability to perform squats at recent follow-up visit.

2.3. Kinematic analysis

Continuous radiographic images of the subjects while squatting were recorded during dynamic movements using a flat-panel X-ray detector (Ultimax-I, Toshiba, Tochigi, Japan), with an image area of 420 mm × 420 mm, resolution of 0.274 mm × 0.274 mm/pixel, 0.02 s pulse width, 80 kV, and 360 mA [20–23]. The frame rate was set at 3.5 frames/s. Subjects were asked to squat with the feet at shoulder width and heels flat from flexed to extended standing positions, and were allowed to squat as they felt comfortable with the given instructions and to warm up sufficiently before data collection (Fig. 1). The 3D positions and orientations of the pelvis and femur while squatting were determined via density-based, 3D-to-2D model-to-image registration techniques with using image correlations (Fig. 2). A 3D digital image was constructed in a virtual 3D space using CT data, and the anatomical coordinate systems of the pelvis and femur were embedded in each density-based volumetric bone model. Thereafter, computer simulation of the radiographic process was conducted to generate virtual digitally reconstructed radiographs (DRRs). Correlations of the pixel values between the DRRs and real X-ray images were used to finetune the 3D model. In particular, multiple image windows that spanned the bone edge were defined for image-matching analysis [20–23].

The upper left end point on the projection plane of a flat panel X-ray detector was defined as the world coordinate system origin. The mediolateral (ML: X) and superoinferior (Y) axis were horizontal and perpendicular to the floor, respectively. The anteroposterior (AP: Z) axis was formed from the cross product of the first two. Anatomical coordinate systems of the pelvis and femur were embedded in each density-based volumetric bone model. The coordinate system of the pelvis was based on the anatomical pelvic plane (APP). The mid-point of the bilateral anterior superior iliac spines was defined as the coordinate system origin for the pelvis. The ML (x) axis of the pelvis was defined by a line passing through
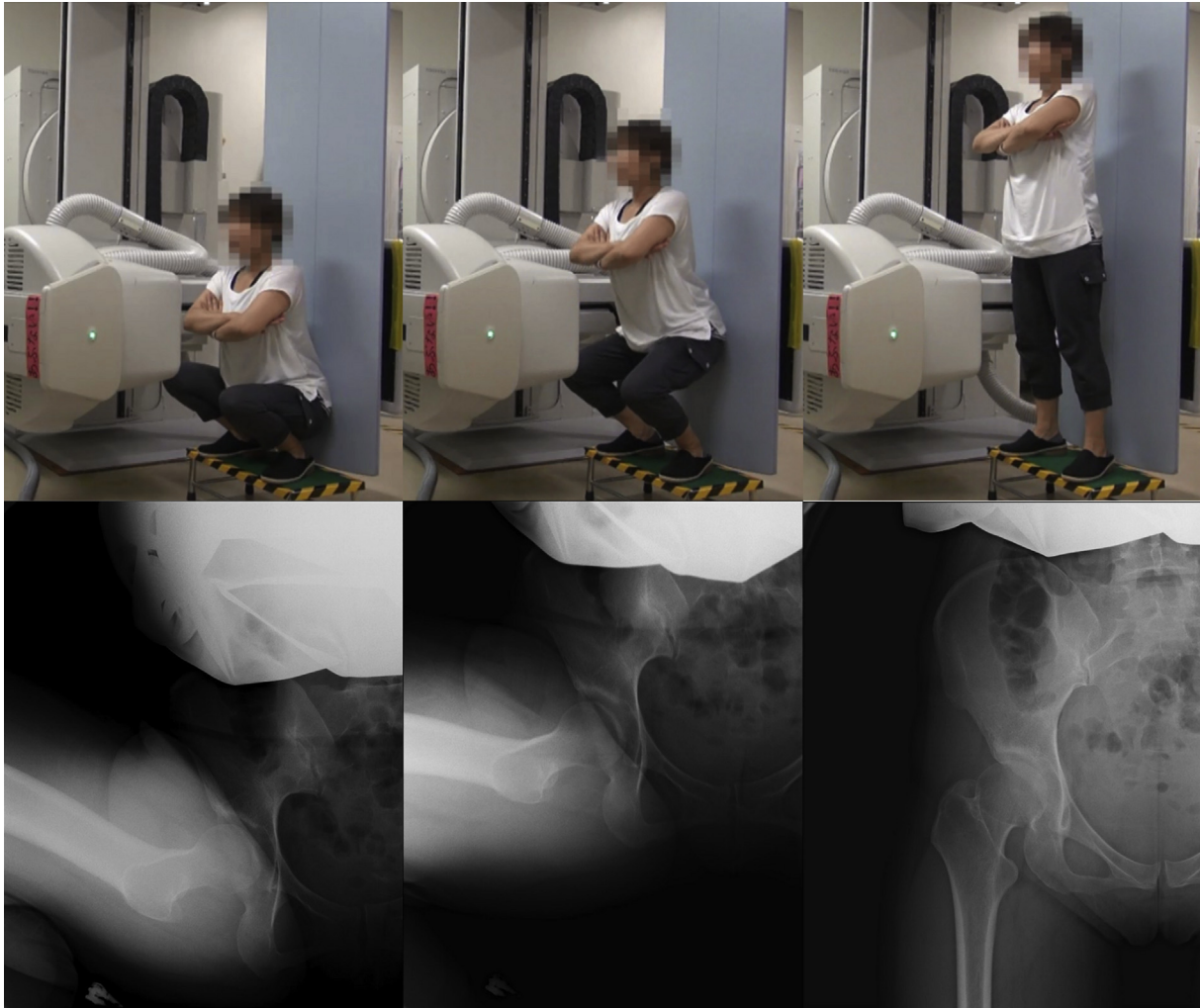
Fig. 1. All the subjects were asked to squat dynamically with the feet at shoulder width and heels flat (upper stand) under radiographic surveillance (lower stand). (A) Flexed position, (B) Middle of squat, and (C) Standing position.

the bilateral anterior superior iliac spines. The proximal/distal (z) axis of the pelvis was defined by a line perpendicular to the x-axis in APP. The AP (y) axis was formed from the cross product of x-and z-axis. The centroid of the femoral head was calculated from the mean position of point clouds of the femoral head in the world coordinate systems, and was defined as the coordinate system origin for the femur. The ML (x) axis of the femur was defined by a line parallel to the trans-epicondylar axis (TEA) in the plane intersecting the origin. The proximal/distal (z) axis of the femur was defined by a line perpendicular to the x-axis in the plane intersecting the origin and the midpoint of TEA. The AP (y) axis was formed from the cross product of x-and z-axis. The relative positions and orientations of the pelvis (anterior/posterior tilt, upward/downward obliquity, contralateral/ipsilateral rotation) and femur (flexion/extension, adduction/abduction, internal/external rotation) with respect to the world coordinate systems were defined as the pelvic and femoral movements. We also defined the relative positions and orientations of the femur to the pelvis as hip movements (flexion/extension, adduction/abduction, internal/external rotation) [20–23].

The distance between the acetabular rim and the femoral neck at maximum hip flexion while squatting was calculated as the rim-neck distance [22,23]. First, pixels of the acetabular rim were plotted in the 3D bone models. Second, the femoral head was approximated as a sphere and was removed from the 3D femoral bone model. The distance between each pixels of the rim and the neck, which was identified by the 3D acetabular and femoral bone models, was calculated by using a computer-aided design software program (CATIA V5; Dassault Systemes, Vélizy-Villacoublay, France), and the minimum distance was determined (Fig. 3).

2.4. Radiographic evaluation

AP pelvic radiographs were obtained in the supine position. In addition, each subject was scanned using CT (Aquilion, Toshiba, Tochigi, Japan) in the supine position with an image matrix of 512×512, pixel dimensions of 0.35×0.35, and a thickness of 1 mm spanning from the superior edge of the pelvis to below the knee joint. Multiplanar reconstruction of all images was performed using image analysis software (3D template; Japan Medical Materials, Osaka, Japan).

On the acetabular side, the sharp angle (SA), acetabular roof obliquity (ARO), and acetabular head index (AHI) were measured using pelvic radiographs. The lateral center-edge angle (LCEA) and ACEA were also measured on coronal and sagittal views of CT images through the femoral head center [34]. A functional pelvic plane in the supine position [35] was defined as the reference plane of the pelvic position. The ACEA, which was calculated based upon CT data in this study, has different meaning comparing with ACEA measured by false profile view radiograph.
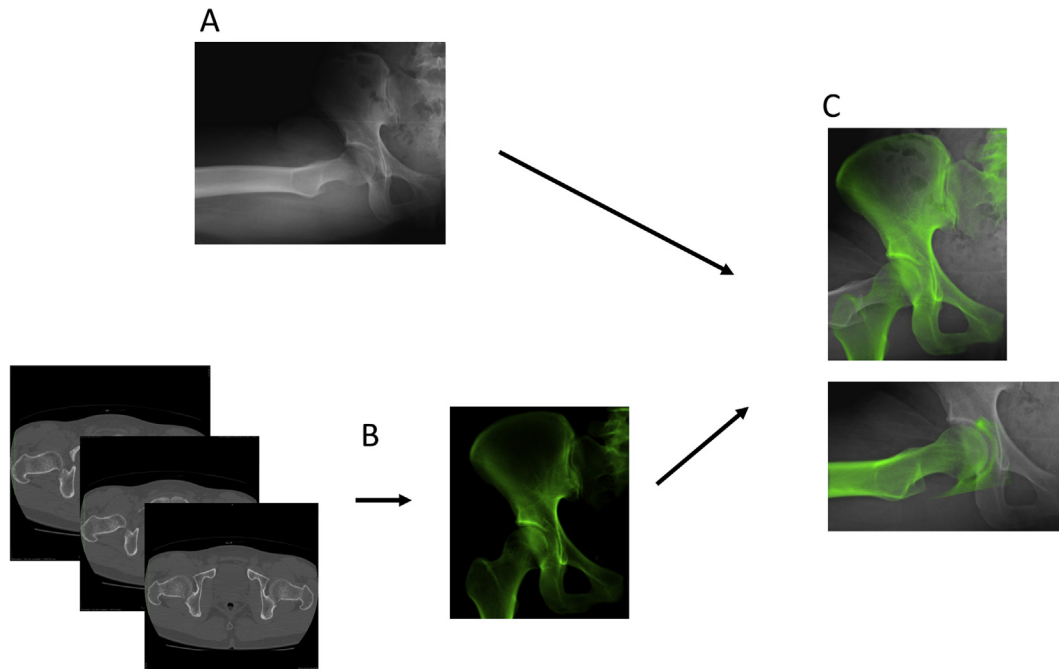
Fig. 2. (A) Hip motions were captured as continuous X-ray images using a flat panel X-ray detector. (B) Computed tomography slices were reconstructed to the density-based digitally reconstructed radiographs. (C) The 6 degrees of freedom for the pelvis and femur were determined by 3D-to-2D model-to-image registration technique with image correlations. Specifically, the dynamic hip motions were captured as continuous X-ray images using a flat panel X-ray detector. CT slices were reconstructed to the density-based digitally reconstructed radiograph (DRR) and projected onto the real X-ray image. Each DRR was matched with the real X-ray image by translating and rotating the 3D model to minimize the number of unmatched pixels between the radiographs.
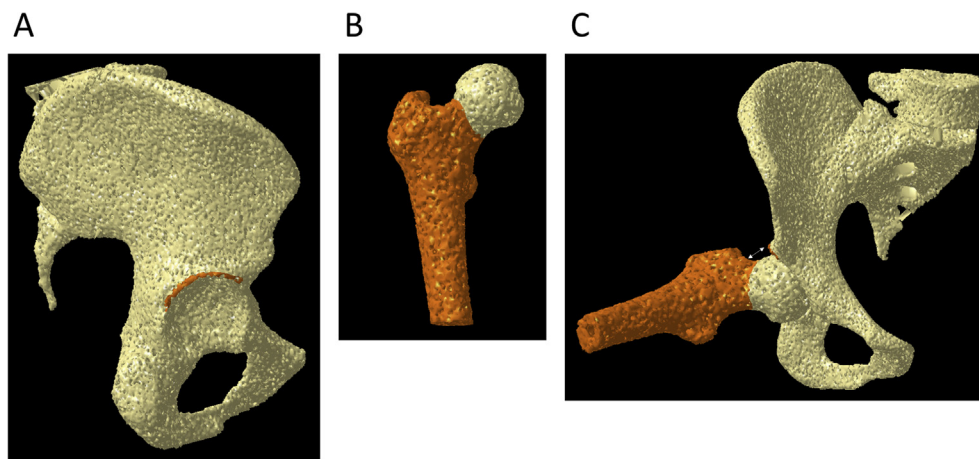

Fig. 3. (A) The pixels of the acetabular rim were plotted on the 3D bone models. (B) The femoral head was approximated as a sphere, and was removed from the 3D femoral bone model. (C) The distance between each pixel of the rim and the femur was calculated as the rim-neck distance.

On the femoral side, the neck-shaft angle (NSA) was measured using pelvic radiographs. The femoral neck anteversion angle (FNA) and α-angle were measured using CT images. A retrocondylar plane [36] was defined as the reference plane of the femur position. To measure the α-angle, multiple radial planes through the femoral neck axes were reconstructed at 30° intervals. The locations were represented by the clock position [37]; the superior aspect was considered as 0 o'clock and the anterior aspect was considered as 3 o'clock. The α-angles from 0 to 3 o'clock were measured because anterior FAI was generally observed from 0 to 3 o'clock [27]. The intraobserver and interobserver correlation coefficients were found to be excellent for the CT measurements, as previously described [37].

2.5. Statistical analysis

Statistical analyses were performed using JMP software version 11.0 (SAS Institute, Cary, NC, USA). Paired t-test was used to compare continuous variables in DDH hips before and after PAO, and Student's t-test was used to compare continuous variables of normal hips and that of DDH hips, whereas χ^2 statistics was used to compare categorical variables. Linear regression analyses were performed to assess whether the acetabular coverage of the femoral head was correlated with hip RoM and the rim-neck distance. A power analysis indicated that a sample size of 14 patients would provide 80% statistical power for detecting a 10° difference in absolute value of RoM between before and after PAO. This

assumes a probability value of less than 0.05 and a standard deviation of 12°.

3. Results

3.1. Kinematics

In normal hips, the maximum hip flexion angles were 102.2° (SD, 14.3) (Fig. 4A). The femoral flexion angles and the pelvic tilt angles (posterior+, anterior−) at maximum hip flexion were 103.3° (SD 12.1) and 1.3° (SD 9.5), respectively (Fig. 4B and C). The hip abduction angles and internal rotation angles at maximum hip flexion were 35.2° (SD, 7.0) and 6.4° (SD, 12.0), respectively (Fig. 4D and E).

In hips with DDH, the maximum hip flexion angles were 100.4° (SD, 18.6) before PAO and 94.9° (SD, 14.0) after PAO (Fig. 4A). The femoral flexion angles at maximum hip flexion were 98.7° (SD, 12.7) before PAO and 97.8° (SD, 9.0) after PAO (Fig. 4B). The pelvic tilt angles (posterior+, anterior−) at maximum hip flexion were

0.4° (SD, 13.5) before PAO and 3.2° (SD, 12.9) after PAO (Fig. 4C). There was no significant difference in maximum hip flexion angles, femoral flexion angles, and pelvic tilt angles at maximum hip flexion before and after PAO (p = 0.0863, 0.1228 and 0.4257, respectively). The hip abduction angles at maximum hip flexion were 31.7° (SD, 12.0) before PAO and 26.2° (SD, 6.3) after PAO (Fig. 4D). The hip internal rotation angles at maximum hip flexion were 3.4° (SD, 11.3) before PAO and 2.8° (SD, 10.8) after PAO (Fig. 4E). There was no significant difference in the hip abduction and hip internal rotation angles at maximum hip flexion before and after PAO (p = 0.1256 and 0.7901). The maximum hip flexion angles, pelvic tilt angles, femoral flexion angles, and hip internal rotation angles at maximum hip flexion after PAO did not significantly differ from those of normal hips (p = 0.2552, 0.7129, 0.2298, and 0.4705, respectively). However, the hip abduction angles at maximum hip flexion after PAO were significantly smaller than those of normal hips (p = 0.0047). When assessing the correlation of acetabular coverage and hip RoM, we found that the ACEA was not significantly correlated with the maximum hip flexion angles
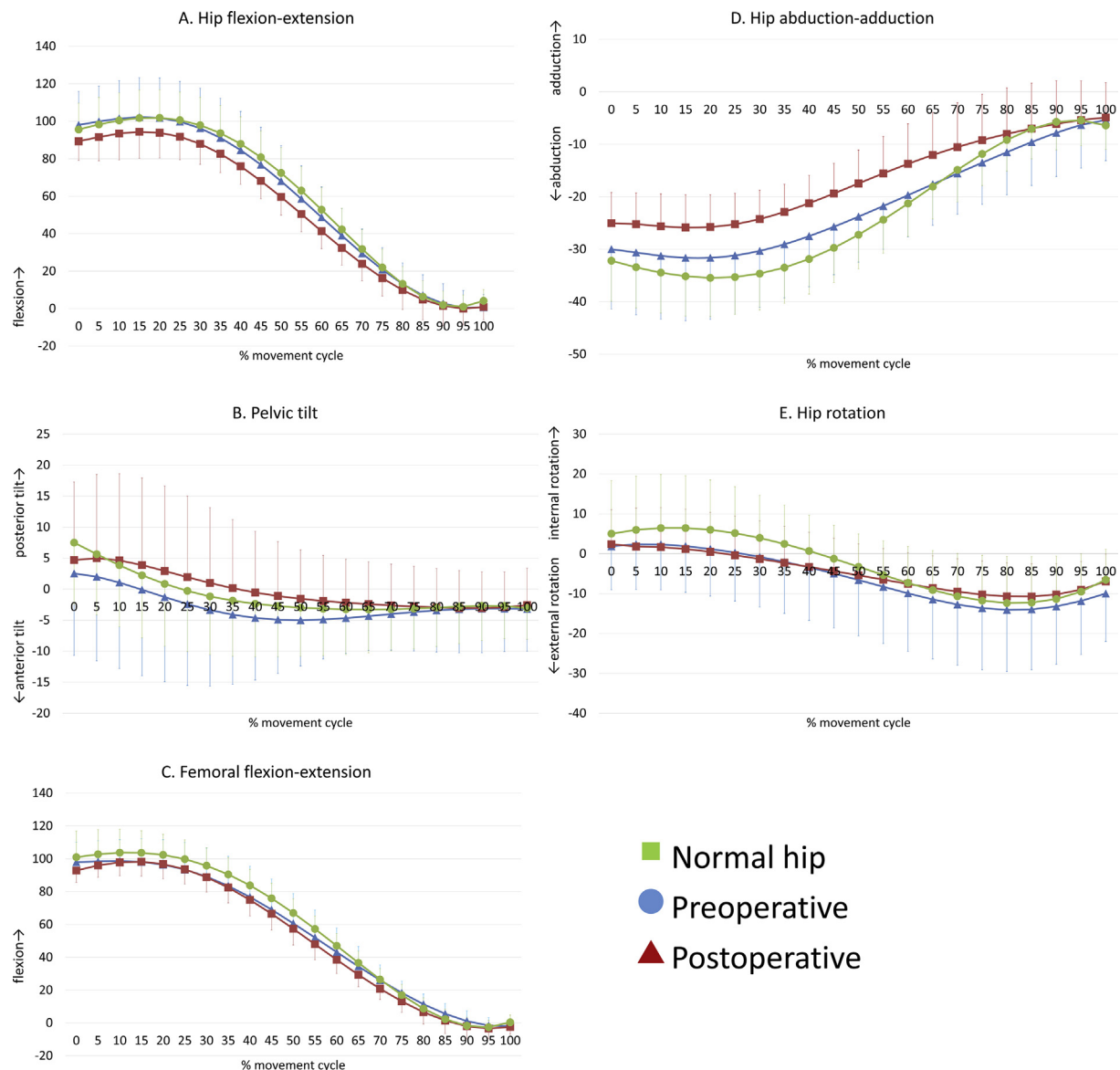

Fig. 4. (A) Femoral flexion-extension angles while squatting. (B) Pelvic tilt angles while squatting. (C) Hip flexion-extension angles while squatting. (D) Hip abduction-adduction angles while squatting. (E) Hip rotation angles while squatting.

(p = 0.9601, r = 0.01), pelvic tilt angles (p = 0.2838, r = 0.18), or hip internal rotation angles (p = 0.7350, r = 0.06) at maximum hip flexion (Fig. 5A, B, C). Moreover, the LCEA was not significantly correlated with the hip abduction angles at maximum hip flexion (p = 0.1683, r = −0.23) (Fig. 5D). The FNA was not correlated with the hip flexion (p = 0.5453, r = −0.10), hip internal rotation (p = 0.5011, r = −0.11) and hip abduction at maximum hip flexion (p = 0.4732, r = 0.12).

3.2. Minimum rim-neck distance

The mean minimum rim-neck distance was 11.3 mm (SD, 5.2) in normal hips, and was 12.2 mm (SD 6.1) before PAO and 8.9 mm (SD 4.6) after PAO in DDH hips. The rim-neck distance was significantly decreased after PAO (p = 0.0044). There was no significant correlation between the ACEA and the rim-neck distance (p = 0.8764, r = 0.03) (Fig. 5E).

3.3. Radiographic evaluation

The LCEA, ACEA, SA, ARO, and AHI in DDH hips improved significantly after PAO (p = 0.0347 for ACEA and p < 0.0001 for the other parameters). The LCEA and AHI after PAO were significantly larger than those of normal hips (p < 0.0001). Moreover, the SA and ARO after PAO were significantly smaller than those of normal hips

(p = 0.0003 and p = 0.0109). However, there were no significant differences between the ACEA after PAO and that of normal hips (p = 0.1917). In all patients with DDH, the ACEA after PAO did not exceed the range of that of normal hips. NSA and FNA were not significantly different between normal hips and DDH hips (p = 0.9521 and 0.4258). At any aspect, there was no significant difference in the α-angle between normal hips and DDH hips (p = 0.1840 at 0′, p = 0.0660 at 1′, p = 0.1146 at 2′ and p = 0.4012 at 3′; Table 1).

4. Discussion

In the present *in vivo* study, we examined the dynamic kinematics of DDH and normal hips while squatting, and assessed the effect of acetabular coverage on hip kinematics. The acetabular coverage of the femoral head improved after PAO, whereas the ACEA after PAO and that of normal hips did not significantly differ. There was no significant difference in maximum hip flexion angles while squatting between before and after PAO, or between patients after PAO and normal hips. Although range of flexion could vary depending on adduction/abduction and internal/external rotation angles, there was no significant difference in the hip abduction and internal rotation angles at maximum hip flexion before and after PAO. The ACEA was not significantly correlated with the hip flexion angles, pelvic tilt, hip internal rotation angles, or the rim-neck distance. The LCEA was also
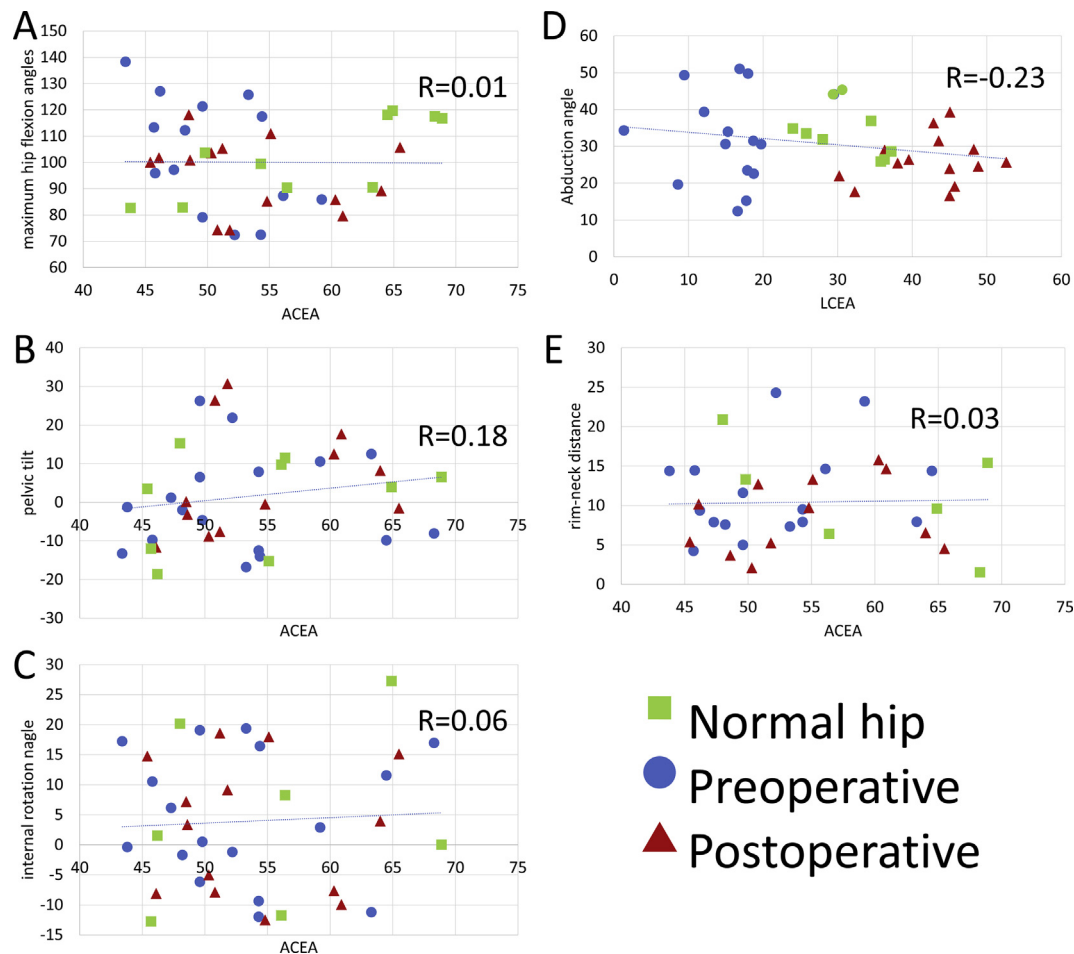

Fig. 5. No significant correlation between the maximum hip flexion angles and the anterior center edge angle (ACEA) is noted (p = 0.9601; A). No significant correlation between the pelvic tilt (p = 0.2838; B), or internal rotation (p = 0.7350; C) angles at maximum hip flexion and the ACEA is noted. No significant correlation between the hip abduction angles at maximum hip flexion and the LCEA is noted (p = 0.2083; D). No significant correlation between the rim-neck distance and the ACEA is noted (p = 0.8764; E). The ACEA and LCEA were calculated based upon a functional pelvic plane of CT data [34,41].

Table 1

Radiographic parameters. The LCEA, ACEA, FNA and α angle were calculated based upon CT data. Functional pelvic and retrocondylar planes were defined as the reference plane of the pelvic and femur positions, respectively.

	Normal hips (n = 10)	DDH (n = 14)	
		Before PAO	After PAO
LCEA (°)	31.1 (SD 4.4)	14.7 (SD 5.0)[b]	42.4 (SD 6.1)[a,c]
ACEA (°)	58.2 (SD 8.5)	50.4 (SD 4.5)[b]	54.0 (SD 6.2)[a]
SA (°)	40.3 (SD 4.0)	47.5 (SD 4.3)[b]	32.1 (SD 4.3)[a,c]
ARO (°)	8.7 (SD 4.2)	15.5 (SD 7.1)[b]	4.0 (SD 3.2)[a,c]
AHI (%)	82.0 (SD 4.9)	67.9 (SD 5.4)[b]	96.4 (SD 3.9)[a,c]
NSA (°)	132.6 (SD 4.4)	133.0 (SD 5.6)	
FNA (°)	23.4 (SD 6.2)	26.9 (SD 11.7)	
α angle 0' (°)	40.2 (SD 5.8)	37.1 (SD 4.9)	
α angle 1' (°)	48.5 (SD 3.6)	43.7 (SD 5.8)	
α angle 2' (°)	49.5 (SD 4.8)	45.1 (SD 7.1)	
α angle 3' (°)	38.8 (SD 2.9)	37.3 (SD 4.6)	

DDH: developmental dysplasia of the hip, PAO: periacetabular osteotomy, LCEA: lateral center edge angle, ACEA: anterior center edge angle, SA: sharp angle, ARO: acetabular roof obliquity, AHI: acetabular hip index, NSA: neck-shaft angle, FNA: femoral neck anteversion angle.

Values are mean (SD: standard deviation).

[a] $p < 0.05$ for the comparison of DDH before and after PAO.

[b] $p < 0.05$ for the comparison of DDH before PAO and normal hips.

[c] $p < 0.05$ for the comparison of DDH after PAO and normal hips.

not significantly correlated with the hip abduction angles. The correction of acetabular coverage through PAO restored hip RoM without coxalgia that induce the inability to perform squats.

In CT based simulation studies, hip flexion, abduction and internal rotation decreased after PAO [17–19], even if the coverage of the femoral head after PAO was close to that of normal hips [34,35]. Furthermore, Iwai et al. [17], in their simulation study, reported that the ACEA was negatively correlated with the hip flexion RoM. They mentioned that increased anterior coverage of the femoral head after PAO induced anterior bony impingement and reduced hip flexion and internal rotation RoM. In the present *in vivo* study, the maximum hip flexion angles before and after PAO were 100.4° and 94.9° without significant difference with those of normal hips: 102.2°. Using an electromagnetic tracking system, Hemmerich et al. [38] reported that mean maximum hip flexion angles reached up to 95° on average for squatting, which is consistent with our results. In this study, the acetabular coverage increased, and the rim-neck distance decreased significantly after PAO. We have previously evaluated kinematics of pincer- and cam-type FAI before and after surgery using image-matching techniques [22,23]. Acetabuloplasty [22] and osteochondroplasty [23] improved the minimum rim-neck distance at maximum hip flexion while squatting from 1.8 to 7.3 mm and from 2.0 to 10.4 mm, respectively. In this study, the mean minimum rim-neck distance was 11.3 mm in normal hips, and was 12.2 mm before PAO and still 8.9 mm after PAO in DDH hips. Although the hip RoM decreased 5.5° on average in both flexion and abduction after PAO without significant difference, acetabular coverage restored hip RoM and rim-neck distance without coxalgia that induce the inability to perform squats. However, the results suggested different kinematics after PAO compared to those of normal hips. Patients after PAO showed the significantly smaller ranges of hip abduction at maximum hip flexion than those of normal hips while squatting. As simulation studies could consider only the influence of bony morphology, increased coverage of the femoral head would directly result in decreasing hip RoM. The present study showed that the influence of soft tissues on hip RoM, in addition to bony morphology, should be carefully considered.

The goals of anterior coverage of the femoral head after PAO remains controversial. In a previous report, a postoperative LCEA of less than 30° or more than 40° was identified as a predictor of

conversion to total hip arthroplasty, with a hazard ratio of 2.0 [39]. Another study identified an LCEA of less than 22° as a predictor of radiographic progression of osteoarthritis with a hazard ratio of 2.2 [40]. Although the goals of LCEA after PAO has been examined, only a few reports have examined the goals of ACEA after PAO. In the present study, we found that modifying the ACEA in patients without cam deformity close to that in normal hips after PAO could yield sufficient flexion RoM while squatting without secondary FAI. The mean ACEA of normal hips calculated through 3D remodeling on the sagittal plane was 58.2° (range, 48.0–64.9; SD, 8.5) in this study, and 58.6° (range, 34.6–73.9) [34,41] in another study. These facts suggested that the goals of ACEA during the procedure could be normalization of ACEA to restore hip RoM or coxalgia that induce the inability to perform squats in patients without cam-type morphology after PAO. Previous studies showed that anterior and lateral overcorrection in the PAO may create secondary FAI with hip flexion disturbance during activities [14,42,43]. Therefore, surgeons should avoid both under and over acetabular coverage of the femoral head during the PAO to obtain successful long-term clinical outcome.

This study has several limitations. First, the number of patients and control subjects included in the study was small, and a larger number of DDH hips and normal subjects would increase the statistical power and could reveal additional kinematic differences, including gender differences. The findings in this study should be interpreted with the understanding that these limitations may significantly bias the results. However, this cohort is similar to that in previous hip kinematic studies (eight healthy and twelve DDH hips [44], eight [45] or eleven [46] replaced hips) due to the demanding study protocol with radiographic surveillances, CT scans, and density-based image-matching techniques, and is consistent with minimizing X-ray exposure to individuals, and the studies nevertheless obtained important information. Second, we only evaluated the kinematics of the hip joint during a squatting. As participation in specific activities requires activity-dependent kinematics, further *in vivo* analyses for other activities of daily living and sport, as well as non-weight-bearing postures, e.g. the anterior and posterior impingement tests, are required. However, squatting is one the most important activity in daily life and is influenced by the coverage of femoral head [22,47], therefore, this study obtained valuable information. Third, we did not examine the reproducibility of the squat because one trial after warm-up was collected from each participant for the analysis to minimize X-ray exposure. To our best knowledge, no previous studies examined quantification of the osseous ROM of the hip before and after PAO during functional weight-bearing activities using objective methods [18].

Patients after PAO showed no significant difference in maximum hip flexion while squatting compared to before PAO and normal hips. Horizontalized weight-bearing acetabulum with normalized ACEA after PAO could be adequate correction of the acetabular fragment to restore hip RoM without coxalgia that induce the inability to perform squats. Anterior and lateral overcorrection in the PAO may create secondary FAI with hip flexion disturbance during activities [15,42,43]. Findings in this study may be useful in the decision-making process of surgeons attempting to correct acetabular coverage during PAO.

Conflict of interest

None.

References

[1] Harris WH. Etiology of osteoarthritis of the hip. Clin Orthop Relat Res 1986 Dec;(213):20–33.

[2] Nishio A. Transposition osteotomy of the acetabulum in the treatment of congenital dislocation of the hip. Nisseikaishi. J Jpn Orthop Assoc 1956;30:483 [in Japanese)].

[3] Matsuo A, Jingushi S, Nakashima Y, Yamamoto T, Mawatari T, Noguchi Y, Shuto T, Iwamoto Y. Transposition osteotomy of the acetabulum for advanced-stage osteoarthritis of the hips. J Orthop Sci 2009 May;14(3):266–73.

[4] Fujii M, Nakashima Y, Yamamoto T, Mawatari T, Motomura G, Iwamoto Y, Noguchi Y. Effect of intra-articular lesions on the outcome of periacetabular osteotomy in patients with symptomatic hip dysplasia. J Bone Jt Surg Br 2011 Nov;93(11):1449–56.

[5] Hamai S, Nakashima Y, Akiyama M, Kuwashima U, Yamamoto T, Motomura G, Ohishi M, Iwamoto Y. Ischio-pubic stress fracture after peri-acetabular osteotomy in patients with hip dysplasia. Int Orthop 2014 Oct;38(10):2051–6.

[6] Hamai S, Kohno Y, Hara D, Shiomoto K, Akiyama M, Fukushi JI, Motomura G, Ikemura S, Fujii M, Nakashima Y. Minimum 10-year clinical outcomes after periacetabular osteotomy for advanced osteoarthritis due to hip dysplasia. Orthopedics 2018 Sep 1;41(5):300–5.

[7] Ninomiya S, Tagawa H. Rotational acetabular osteotomy for the dysplastic hip. J Bone Jt Surg Am 1984 Mar;66(3):430–6.

[8] Nakamura S, Ninomiya S, Takatori Y, Morimoto S, Umeyama T. Long-term outcome of rotational acetabular osteotomy: 145 hips followed for 10-23 years. Acta Orthop Scand 1998 Jun;69(3):259–65.

[9] Ganz R, Klaue K, Vinh TS, Mast JW. A new periacetabular osteotomy for the treatment of hip dysplasias. Technique and preliminary results. Clin Orthop Relat Res 1988 Jul;(232):26–36.

[10] Hasegawa Y, Iwase T, Kitamura S, Yamauchi Ki K, Sakano S, Iwata H. Eccentric rotational acetabular osteotomy for acetabular dysplasia: follow-up of one hundred and thirty-two hips for five to ten years. J Bone Joint Surg Am 2002 Mar;84-A(3):404–10.

[11] Naito M, Shiramizu K, Akiyoshi Y, Ezoe M, Nakamura Y. Curved periacetabular osteotomy for treatment of dysplastic hip. Clin Orthop Relat Res 2005 Apr;(433):129–35.

[12] Yasunaga Y, Ochi M, Yamasaki T, Adachi N. Rotational acetabular osteotomy. JBJS Essent Surg Tech 2017 Dec 13;7(4):e36.

[13] Kaneuji A, Sugimori T, Ichiseki T, Fukui K, Takahashi E, Matsumoto T. Rotational acetabular osteotomy for osteoarthritis with acetabular dysplasia: conversion rate to total hip arthroplasty within twenty years and osteoarthritis progression after a minimum of twenty years. J Bone Joint Surg Am 2015 May 6;97(9):726–32.

[14] Myers SR, Eijer H, Ganz R. Anterior femoroacetabular impingement after periacetabular osteotomy. Clin Orthop Relat Res 1999 Jun;(363):93–9.

[15] Clohisy JC, Nunley RM, Carlisle JC, Schoenecker PL. Incidence and characteristics of femoral deformities in the dysplastic hip. Clin Orthop Relat Res 2009 Jan;467(1):128–34.

[16] Nassif NA, Schoenecker PL, Thorsness R, Clohisy JC. Periacetabular Osteotomy and Combined Femoral head-neck junction osteochondroplasty: a minimum two-year follow-up cohort study. J Bone Joint Surg Am 2012 Nov 7;94(21):1959–66.

[17] Iwai S, Kabata T, Maeda T, Kajino Y, Watanabe S, Kuroda K, Fujita K, Hasegawa K, Tsuchiya H. Three-dimensional kinetic simulation before and after rotational acetabular osteotomy. J Orthop Sci 2014 May;19(3):443–50.

[18] Steppacher SD, Zurmühle CA, Puls M, Siebenrock KA, Millis MB, Kim Y-J, Tannast M. Periacetabular osteotomy restores the typically excessive range of motion in dysplastic hips with a spherical head. Clin Orthop Relat Res 2015 Apr;473(4):1404–16.

[19] Hamada H, Takao M, Nakahara I, Sakai T, Nishii T, Sugano N. Hip range-of-motion (ROM) is less than normal after rotational acetabular osteotomy for developmental dysplasia of the hip. A simulated ROM analysis. J Orthop Res 2016 Feb;34(2):217–23.

[20] Hara D, Nakashima Y, Hamai S, Higaki H, Ikebe S, Shimoto T, Hirata M, Kanazawa M, Kohno Y, Iwamoto Y. Kinematic analysis of healthy hips during weight-bearing activities by 3D-to-2D model-to-image registration technique. BioMed Res Int 2014:457573–8.

[21] Hara D, Nakashima Y, Hamai S, Higaki H, Ikebe S, Shimoto T, Yoshimoto K, Iwamoto Y. Dynamic hip kinematics in patients with hip osteoarthritis during weight-bearing activities. Clin Biomech 2016 Feb;32:150–6.

[22] Yoshimoto K, Hamai S, Higaki H, Gondo H, Ikebe S, Nakashima Y. Pre- and post-operative evaluation of pincer-type femoroacetabular impingement during squat using image-matching techniques: a case report. Int J Surg Case Rep 2018;42:121–7.

[23] Yoshimoto K, Hamai S, Higaki H, Gondoh H, Nakashima Y. Visualization of a cam-type femoroacetabular impingement while squatting using image-matching techniques: a case report. Skeletal Radiol 2017 Sep;46(9):1277–82.

[24] Wiberg G. Studies on dysplastic acetabula and congenital subluxation of the hip joint : with special reference to the complication of osteoarthritis. Acta Chir Scand 1939;83(Suppl 58):7–38.

[25] Crowe JF, Mani VJ, Ranawat CS. Total hip replacement in congenital dislocation and dysplasia of the hip. J Bone Joint Surg Am 1979 Jan;61(1):15–23.

[26] Irie T, Takahashi D, Asano T, Arai R, Terkawi MA, Ito YM, Iwasaki N. Is there an association between borderline-to-mild dysplasia and hip osteoarthritis? Analysis of CT osteoabsorptiometry. Clin Orthop Relat Res 2018 Jul;476(7):1455–65.

[27] Fujii M, Nakashima Y, Yamamoto T, Mawatari T, Motomura G, Matsushita A, Jingushi S, Iwamoto Y. Acetabular retroversion in developmental dysplasia of the hip. J Bone Joint Surg Am 2010 Apr;92(4):895–903.

[28] Ito H, Matsuno T, Hirayama T, Tanino H, Yamanaka Y, Minami A. Three-dimensional computed tomography analysis of non-osteoarthritic adult acetabular dysplasia. Skeletal Radiol 2009 Feb;38(2):131–9.

[29] Fujii M, Nakashima Y, Sato T, Akiyama M, Iwamoto Y. Pelvic deformity influences acetabular version and coverage in hip dysplasia. Clin Orthop Relat Res 2011 Jun;469:1735–42.

[30] Fujii M, Nakashima Y, Sato T, Akiyama M, Iwamoto Y. Acetabular tilt correlates with acetabular version and coverage in hip dysplasia. Clin Orthop Relat Res 2012 Oct;470(10):2827–35.

[31] Johnston 2nd CE, Wenger DR, Roberts JM, Burke SW, Roach JW. Acetabular coverage: three-dimensional anatomy and radiographic evaluation. J Pediatr Orthop 1986 Sep-Oct;6(5):548–58.

[32] Azuma H, Taneda H, Igarashi H, Fujioka M. Preoperative and postoperative assessment of rotational acetabular osteotomy for dysplastic hips in children by three-dimensional surface reconstruction computed tomography imaging. J Pediatr Orthop 1990 Jan-Feb;10(1):33–8.

[33] Peters CL, Erickson JA, Anderson L, Anderson AA, Weiss J. Hip-preserving surgery: understanding complex pathomorphology. J Bone Joint Surg Am 2009 Nov;91(Suppl 6):42–58.

[34] Dandachli W, Najefi A, Iranpour F, Lenihan J, Hart A, Cobb J. Quantifying the contribution of pincer deformity to femoro-acetabular impingement using 3D computerised tomography. Skeletal Radiol 2012 Sep;41(10):1295–300.

[35] Nakahara I, Takao M, Sakai T, Nishii T, Yoshikawa H, Sugano N. Gender differences in 3D morphology and bony impingement of human hips. J Orthop Res 2011 Mar;29(3):333–9.

[36] Kingsley PC, Olmsted KL. A study to determine the angle of anteversion of the neck of the femur. J Bone Joint Surg Am 1948 Jul;30A(3):745–51.

[37] Kohno Y, Nakashima Y, Hatano T, Akiyama M, Fujii M, Hara D, Kanazawa M, Haraguchi A, Iwamoto Y. High prevalence of cam deformity in dysplastic hips: a three-dimensional CT study. J Orthop Res 2016 Sep;34(9):1613–9.

[38] Hemmerich A, Brown H, Smith S, Marthandam SS, Wyss UP. Hip, knee, and ankle kinematics of high range of motion activities of daily living. J Orthop Res 2006 Apr;24(4):770–81.

[39] Hartig-Andreasen C, Troelsen A, Thillemann TM, Søballe K. What factors predict failure 4 to 12 years after periacetabular osteotomy? Clin Orthop Relat Res 2012 Nov;470(11):2978–87.

[40] Albers CE, Steppacher SD, Ganz R, Tannast M, Siebenrock KA. Impingement adversely affects 10-year survivorship after periacetabular osteotomy for DDH. Clin Orthop Relat Res 2013 May;471(5):1602–14.

[41] Nakahara I, Takao M, Sakai T, Miki H, Nishii T, Sugano N. Three-dimensional morphology and bony range of movement in hip joints in patients with hip dysplasia. Bone Joint Lett J 2014 May;96-B(5):580–9.

[42] Siebenrock KA, Schöll E, Lottenbach M, Ganz R. Bernese periacetabular osteotomy. Clin Orthop Relat Res 1999 Jun;(363):9–20.

[43] Steppacher SD, Tannast M, Werlen S, Siebenrock KA. Femoral morphology differs between deficient and excessive acetabular coverage. Clin Orthop Relat Res 2008 Apr;466(4):782–90.

[44] Sato T, Tanino H, Nishida Y, Ito H, Matsuno T, Banks SA. Dynamic femoral head translations in dysplastic hips. Clin Biomech (Bristol, Avon) 2017 Jul;46:40–5.

[45] Tsai T-Y, Dimitriou D, Li J-S, Woo Nam K, Li G, Kwon Y-M. Asymmetric hip kinematics during gait in patients with unilateral total hip arthroplasty: in vivo 3-dimensional motion analysis. J Biomech 2015 Feb 26;48(4):555–9.

[46] Hara D, Nakashima Y, Hamai S, Higaki H, Ikebe S, Shimoto T, Hirata M, Kanazawa M, Kohno Y, Iwamoto Y. Dynamic hip kinematics during golf swing in patients after total hip arthroplasty. Am J Sports Med 2016 Jul;44(7):1801–9.

[47] Philippon MJ, Maxwell RB, Johnston TL, Schenker M, Briggs KK. Clinical presentation of femoroacetabular impingement. Knee Surg Sports Traumatol Arthrosc 2007 Aug;15(8):1041–7.